JOURNAL OF SOLID STATE CHEMISTRY 33, 283–288 (1980)

High-Pressure/High-Temperature Phase Relations and Vibrational Spectra of $CsSbF_6$

W. H. J. DE BEER* AND ANTON M. HEYNS

Department of Physical Chemistry, University of South Africa, P.O. Box 392, Pretoria, South Africa

AND P. W. RICHTER AND J. B. CLARK

National Physical Research Laboratory, South African Council for Scientific and Industrial Research, P.O. Box 395, Pretoria, South Africa

Received June 29, 1979; in revised form September 12, 1979

$CsSbF_6$(II) under ambient conditions is trigonal, space group D_{3d}^5–$R\bar{3}m$. At 187.8°C it undergoes a phase transition with an enthalpy change of 5.267 ± 0.316 kJ mole^{-1}, to phase $CsSbF_6$(I). $CsSbF_6$ decomposes with loss of fluorine at atmospheric pressure at high temperatures, but under pressure the decomposition is prevented and a melting point of 310°C at atmospheric pressure can be inferred. The II/I phase boundary and melting curve were studied as functions of pressure. The infrared and Raman spectra of $CsSbF_6$(II) were studied in the temperature range of −256 to 20°C, at ambient pressure. The crystal chemistry of the $CsSbF_6$ and its relationship with other related compounds is discussed.

Introduction

The high-pressure phase relations, vibrational spectra, and crystal chemistry have been presented for KPF_6 (*1*), $KAsF_6$ (*2*), $KSbF_6$ (*3*), and $NaPF_6$ (*4*).

$CsSbF_6$ is reported (*5*) to be trigonal with space group D_{3d}^5–$R\bar{3}m$ at ambient temperature. The structure can be thought of as an arrangement of Cs^+ and SbF_6^- ions in a distorted CsCl configuration.

The vibrational spectra of the SbF_6^- ion have been studied extensively (*3, 6*); however, only a portion of the infrared spectrum of $CsSbF_6$ has been reported (*7*).

The present investigation reports the phase behavior of $CsSbF_6$ between −256°C and the melting point at 310°C. Phase behavior at high pressure and high temperature is also reported. Finally, infrared, far-infrared, and Raman spectra are reported from −256 to 20°C.

Experimental

The $CsSbF_6$ was prepared from Sb_2O_5, Cs_2CO_3, and an excess of hydrofluoric acid using the method described by Kolditz and Rehak (*8a*). Antimony was determined iodometrically according to Mazeika and Neumann (*8b*) after addition of boric acid. The fluorine content was determined by the methods described by Palmer (*9*) and Vogel (*10*). The chlorine is determined by Volhard's method from which the fluorine

* Permanent address: Department of Chemistry, Pretoria Technikon, 420 Church Street, Pretoria, South Africa.

0022-4596/80/090283-06$02.00/0

can be calculated. An Sb:F value of 1:5.95 was found.

X-Ray powder diffraction patterns for identification and comparison were recorded on a Huber Guinier camera using monochromatized Cu$K\alpha_1$ radiation (λ = 1.54051 Å). Si was used as an internal calibrant and both film and counter techniques were employed. The diffraction pattern obtained agreed with that reported in the ASTM file (*11*).

The thermal behavior of $CsSbF_6$ at temperatures above room temperature was determined by DSC techniques on a DuPont 990 thermal analyzer. Heating rates varied between 2 and 5°C min^{-1}. The sensitivity of the calorimeter varied between 0.1 and 1 mcal sec^{-1}. Peak areas were used to calculate enthalpy values. All temperatures and enthalpy measurements were calibrated with respect to indium and lead standards.

Pressure was generated in a piston-cylinder device (*12*). Phase transitions were detected by differential thermal analysis (DTA), using Chromel–Alumel thermocouples. Experimental techniques have been described in detail elsewhere (*13, 14*). Oven assemblies were constructed of talc. Samples were contained in nickel capsules with no evidence of contamination.

The infrared spectra were recorded in the form of KBr pellets or nujol or mineral oil mulls on KBr, CsBr, or CsI windows, using a Perkin–Elmer Model 621 spectrophotometer. Polyethylene windows were used for the recording of the far-infrared spectra on a Beckmann FS 720 interferometer. These spectra were recorded with a resolution of 2 cm^{-1}. Low-temperature infrared and far-infrared spectra were obtained by means of a RIIC variable temperature unit.

The Raman spectra were recorded on a Spex Ramalog instrument consisting of a double spectrometer Model 1401 equipped with photon counting electronics and a thermoelectrically cooled FW 130 photomultiplier. The excitation source was the

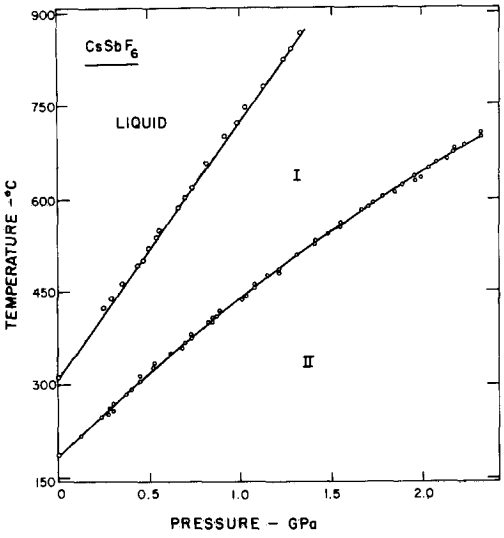

FIG. 1. The phase diagram of $CsSbF_6$.

4880-Å line of a coherent radiation Ar^+-ion laser at a strength of about 50 mW at the sample. The spectral slit width used in the measurements was 2 cm^{-1}. For the low-temperature Raman spectra a Spectrim TM Cryocooler, obtained from Cryogenic Technology, Inc., was used to cool the samples down to 17 K.

Results

Thermal Studies at Atmospheric Pressure

A solid–solid transition was discovered

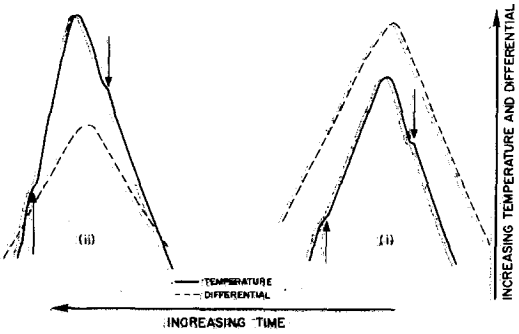

FIG. 2. Typical DTA signals obtained for $CsSbF_6$ on: (i) II/I boundary at 1.84 GPa, 615°C; (ii) I/liquid boundary at 0.82 GPa, 654°C.

TABLE I

CORRELATION BETWEEN THE POINT O_h AND SITE GROUP D_{3d} SYMMETRIES

O_h	D_{3d}
ν_1–A_{1g} (R)	$A_{1g}(xx + yy, zz)$
ν_2–E_g (R)	$E_g(xx - yy, xy), (xz, yz)$
ν_3, ν_4–F_{1u} (ir)	A_{2u} (T_z)
	$E_u(T_x, T_y)$
ν_5–F_{2g} (R)	A_{1g} $(xx + yy, zz)$
	$E_g(xx - yy, xy), (xz, yz)$
ν_6–F_{2u}	A_{1u}
	$E_u(T_x, T_y)$

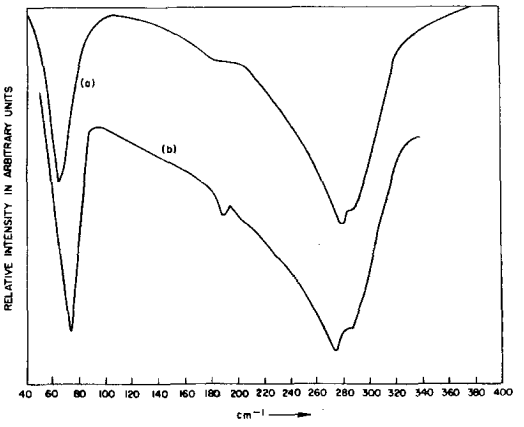

FIG. 3. Far-infrared spectra of $CsSbF_6$ at (a) 20°C and (b) −190°C.

at 187.8°C with an enthalpy change of 5.267 ± 0.316 kJ mole^{-1}. At temperatures of approximately 310°C melting occurred with simultaneous decomposition and loss of fluorine. The fluorine was identified by its characteristic odor, attack on glass and aluminum capsules, and X-ray diffraction examination of products upon cooling. The products were identified as antomony oxide and cesium fluoride.

High-Pressure Studies

The high-pressure phase diagram of $CsSbF_6$ is shown in Fig. 1. Typical DTA signals obtained on the II/I boundary are shown in Fig. 2i. The II/I transition boundary rises steeply with an initial slope of 274.36°C GPa^{-1} and was followed to ~2.3 GPa. The data obtained can be described by:

$$t(°C) = 187.8 + 274.36\,P - 22.345\,P^2 \quad (P \text{ in GPa}),$$

with a standard deviation of 4.9°C. On steep phase boundaries the major experimental uncertainty is a pressure uncertainty and this translates into a relatively high temperature standard deviation.

Under high pressure, the decomposition upon melting was initially suppressed. The melting curve could therefore be determined to ~1.3 GPa where $CsSbF_6$ melts at ~868°C. At higher pressures, and more important, higher temperatures, clear evidence was found that $CsSbF_6$ decomposed. For this reason only data below 1.3 GPa are reported. Typical DTA signals obtained on the melting curve are shown in Fig. 2ii. The melting curve also rises steeply with increasing pressure with an initial slope of 427.6°C GPa^{-1}. The data can be described by:

$$t(°C) = 310.0 + 427.6P \ (P \text{ in GPa}),$$

with a standard deviation of 10.8°C.

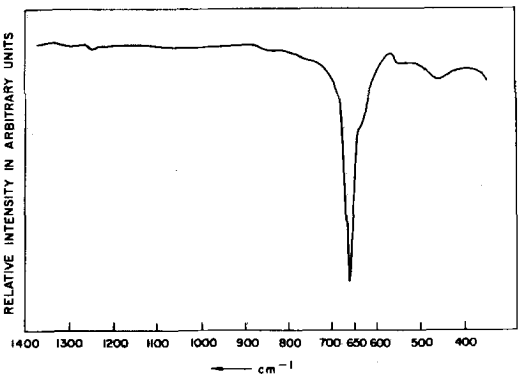

FIG. 4. Infrared spectra of $CsSbF_6$ at −190°C. The spectra at 20°C showed no changes.

TABLE II

INFRARED SPECTRA OF $CsSbF_6$ AT 20 AND −190°C

20°C	−190°C	Assignment	Calculated (20°C) (cm^{-1})
1300 w	1300 w	$\nu_1 + \nu_3$	1280–1320
1260 w	1260 w	$\nu_1 + \nu_3$	1280–1320
950 w	960 w	$\nu_3 + \nu_5$	933–952
845 w	855 w	$\nu_2 + \nu_4$	840–852
668 sh	670 sh	ν_3	
655 s	658 s	ν_3	
635 sh	640 sh	$\nu_2 + \nu_{1_L}$	630–640
560 w	560 w	$\nu_5 + \nu_4$	556–565
450 w	450 w	$\nu_5 + \nu_6$	450–473
288 sh	285 sh	ν_4	
280 s	276 s	ν_4	
180–195 sh	188 w	ν_6	
66 s	74 s	ν_{1_L}	

Crystallography

$CsSbF_6$(II) is reported to be trigonal, space group D_{3d}^5–$R\bar{3}m$ with a = 7.9026 Å and c = 8.2525 Å. The present Guinier powder X-ray diffraction results yielded a = 7.9037 Å and c = 8.2543 Å, in excellent agreement with the ASTM data (*11*).

Vibrational Spectra of $CsSbF_6$(*II*)

Under D_{3d}^5 symmetry, the site group symmetries of both the Cs^+ and SbF_6^- ions are D_{3d} and the correlation between the O_h-point group symmetry of the "free" SbF_6^- ions and the site and unit-cell group symmetry of D_{3d} is shown in Table I (*15*).

The infrared spectra of $CsSbF_6$(II) are shown in Figs. 3 and 4 and these results are summarized and the absorption bands are assigned in Table II. The assignment of the infrared bands is done by analogy to previous studies of the SbF_6^- ion (*3, 6*); however, the bands are relatively broad even at lower temperatures and it is therefore difficult to determine whether the infrared active modes ν_3 and ν_4 are split. It does appear as if there is a broad and sometimes ill-defined shoulder on the high-frequency wings of both these modes. In comparison with the infrared bands, the Raman-active vibrations ν_1, ν_2, and ν_5 (see Table III) are narrow and well-defined bands (Fig. 5) and the A_{1g}–E_g splitting of ν_5 is clearly evident even at room temperature. At 17 K, the modes ν_2, ν_{5a}, and ν_{5b} shift to slightly higher frequencies, but no additional components can be discerned and it is therefore shown that $CsSbF_6$(II) does not undergo any additional phase transitions at low temperatures. We were unfortunately unable to grow large single crystals of $CsSbF_6$(II) but we have recorded polarized Raman spectra of small single crystals of this compound. They were too small to obtain good polarized data. However, the spectra distinctly showed that the 276 cm^{-1} component of ν_5 belongs to the A_{1g} symmetry, whereas the 283 cm^{-1} component belongs to the E_g symmetry.

TABLE III

RAMAN SPECTRA OF $CsSbF_6$ AT 20 AND −256°C

20°C			−256°C			Assignment
cm^{-1}	RI	HW (cm^{-1})	cm^{-1}	RI	HW (cm^{-1})	
650	100	5	651	100	3	ν_1
570	13	6	576	14	3	ν_2
283	40	4	288	30	4	ν_5
276	26	4	279	20	5	ν_5

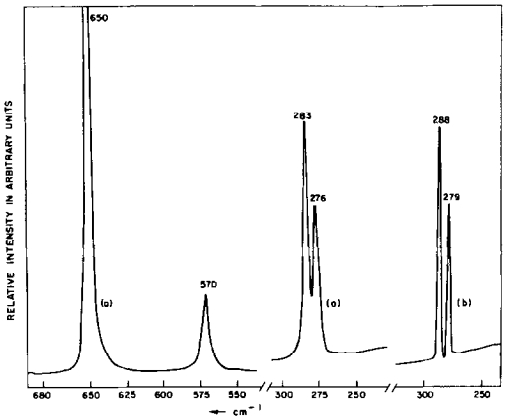

FIG. 5. Raman spectra of polycrystalline $CsSbF_6$ at (a) 20°C and (b) −256°C.

The infrared-inactive mode ν_6 under O_h symmetry is activated under D_{3d} symmetry and a broad shoulder can de discerned at 180–195 cm^{-1} at room temperature (Table II), which is in agreement with the frequency region in which ν_6 was previously reported to occur (*3*). At lower temperatures a relatively distinct component is observed at 188 cm^{-1}, which is in agreement with the predictions in the correlation table, viz., ν_6 is observed not to be split.

The rotational motions of the SbF_6^- ions form the presentation $\Gamma_{rot} = A_{2g}(-) + E_g$ (R) and the translational modes form the representation $\Gamma_{trans} = A_{2u}$ (infrared) + E_u (infrared). It is therefore possible to observe an E_g rotational mode in the Raman spectrum of $CsSbF_6$ and two translation modes in the infrared spectra. Unfortunately, fluorescence was always present in the Raman spectra of $CsSbF_6$(II) at lower frequencies, with the result that reliable spectra could not be obtained below ~100 cm^{-1}; since the rotational mode of the SbF_6^- ion has previously been reported to occur at ~70 cm^{-1} in $TlSbF_6$ (*16*), it is possible that this mode was obscured by fluorescence effects in $CsSbF_6$(II). In the case of the translational modes, Fig. 3 shows that a very well-defined peak is observed at 66 cm^{-1} at room temperature, which shifts upward to 74 cm^{-1} upon cooling of the sample to 90 K.

However, this band remains single at lower temperatures and it is therefore possible either that the second component of the translational mode is too weak in order to be observed, or that it lies at very low frequencies and could therefore not be observed in the present work.

Discussion

The vibrational spectra of $CsSbF_6$(II) are very typical of those of RMX_6 crystals with unimolecular rhombohedral cells (*2, 16*) which can be regarded as slightly distorted arrangements of CsCl. These spectra exhibit single Raman lines for ν_1 and ν_2 but ν_5 is very distinctly split into the predicted A_{1g}–E_g components under $D_{3d}{}^5$. $TlSbF_6$ has the identical structure of $CsSbF_6$(II) and it is therefore not unexpected that their Raman spectra show a close correspondence. In $TlSbF_6$ the A_{1g}–E_g splitting of ν_5 amounts to 13 cm^{-1}, compared with the corresponding amount of 7 cm^{-1} in $CsSbF_6$(II) at room temperature, which increases only slightly to 9 cm^{-1} at −256°C. These results probably point to a lesser distortion of the SbF_6^- ion in $CsSbF_6$(II) than in $TlSbF_6$. The frequencies of the two remaining Raman-active modes, viz., ν_1 and ν_2 agree within ±4 cm^{-1} in the two compounds. On the other hand, the infrared absorption peaks are relatively broad with the result that the A_{2u}–E_u splittings are not so obvious, as is evident in Figs. 3 and 4. In ν_3, in particular, the occurrence of any weak features which can possibly be attributed to this splitting is masked by the appearance of combination bands. The occurrence of ν_6 as a single band supports the $D_{3d}{}^5$ structure for $CsSbF_6$.

Using the experimental values obtained for the transition enthalpy and slope of the I/II transition one can calculate a volume

change of 0.3 cm^3 $mole^{-1}$. $CsSbF_6$(II) has a B2-related structure and the question arises as to the nature of $CsSbF_6$(I). The $CsSbF_6$(I/II) transition has a steep initial slope, viz., 274.4°C GPa^{-1} which is similar to that obtained for the KPF_6(I/II) transition, viz., 211°C GPa^{-1}. It is therefore tempting to assume that the $CsSbF_6$(I) phase may be B1 related as in the case of KPF_6(I). This is almost certainly not the case due to the low volume change associated with the $CsSbF_6$(I/II) transition, viz., 0.3 cm^3 $mole^{-1}$ compared with 4.9 cm^3 $mole^{-1}$ for the KPF_6(I/II) transition. The $CsSbF_6$(I/II) transition therefore probably has more order–disorder character with the high-temperature $CsSbF_6$(I) phase remaining B2 related.

Acknowledgments

The authors would like to thank Mr. A. I. Kingon for valuable discussions. Calculations were carried out on the IBM System 360/65H of the National Research Institute for Mathematical Sciences. One of the authors, A. M. Heyns, wishes to thank the CSIR for financial support.

References

1. A. M. Heyns and C. W. F. T. Pistorius, *Spectrochim. Acta Part A* **30**, 99 (1974).
2. A. M. Heyns and C. W. F. T. Pistorius, *Spectrochim. Acta Part A* **31**, 1293 (1975).
3. A. M. Heyns and C. W. F. T. Pistorius, *Spectrochim. Acta Part A* **32**, 535 (1976).
4. A. M. Heyns and C. W. F. T. Pistorius, P. W. Richter, and J. B. Clark, *Spectrochim. Acta Part A* **34**, 279 (1978), and correction note to be published.
5. N. Schrewelius, *Ark. Kemi Mineral. Geol.* **16B**, 1 (1943).
6. G. M. Begun and A. C. Rutenberg, *Inorg. Chem.* **6**, 2212 (1967).
7. E. Thilo, *Z. Chem.* **3**, 312 (1963).
8. (*a*) V. L. Kolditz and W. Rehak, *Z. Anorg. Allg. Chem.* **300**, 322 (1959).
8. (*b*) W. A. Mazeika and H. M. Neumann, *Inorg. Chem.* **5**, 309 (1966).
9. W. G. Palmer, *in* "Experimental Inorganic Chemistry," p. 306, Cambridge (1970).
10. A. I. Vogel (Ed.), *in* "A Textbook of Quantitative Inorganic Analysis," 3rd ed., p. 269, Longman, New York (1961).
11. "Index: Powder Diffraction File," pp. 15–808, ASTM, York, Pa. (1978).
12. G. C. Kennedy and P. N. Lamori, *in* "Progress in Very High Pressure Research" (F. P. Bundy, W. R. Hibbard, and H. M. Strong, Eds.), pp. 304–313, Wiley, New York (1961).
13. P. W. Richter and C. W. F. T. Pistorius, *J. Solid State Chem.* **3**, 197 (1971).
14. C. W. F. T. Pistorius and J. B. Clark, *High Temp. High Pressures* **1**, 561 (1969).
15. W. G. Fateley, F. R. Dollish, W. R. McDevitt, and F. F. Bentley, "Infrared and Raman Selection Rules for Molecular and Lattice Vibrations—The Correlation Method," Wiley–Interscience, New York (1972).
16. D. Breitinger and U. Kristen, *J. Solid State Chem.* **22**, 233 (1977).